International Journal of Research and Technology in Electrical Industry

journal homepage: ijrtei.sbu.ac.ir

Shahid Beheshti University

# Attitude fault tolerant control of the satellite with four reaction wheels using super twisting sliding mode control

Hossein Moladavoudi[1], Zeinab Talebi[2], Mojtaba Nouri Manzar[1*]

[1] *Electrical Engineering Faculty, Shahid Beheshti University, Tehran, Iran*
[2] *Iran Space Institute, Tehran, Iran*

ARTICLE INFO

**Article history:**
Received: 09 December 2024
Revised: 27 January 2025
Accepted: 30 January 2025

**Keywords:**
Super twisting sliding mode control
External disturbances
Sliding observer
Uncertainty in the inertial matrix
Fault tolerant control



ABSTRACT

In this paper, an adaptive super-twisting sliding mode fault-tolerant control (FTC) method is proposed to control the attitude of a satellite with four reaction wheels. This method has several advantages, such as preventing singularity phenomena, achieving convergence in finite time, and reducing the chattering phenomenon. Additionally, a sliding adaptive fault estimation mechanism is designed to estimate actuator faults, including complete failures, despite the influence of external disturbances and uncertainties in the satellite's attitude dynamics. Furthermore, an optimal control allocation scheme is employed to distribute the control signal to the actuators in real-time, even in the presence of faults, failures, and some limitations. To increase the accuracy of the model, the dynamics of the actuators, which have a pyramid configuration, are incorporated into the dynamics of the satellite's attitude. The stability of the closed-loop system with the proposed controller is analyzed using the Lyapunov method. Finally, the effectiveness of the proposed method is confirmed through simulations and comparisons with a traditional sliding mode method.

## 1. Introduction

Attitude control is the task of determining, stabilizing, and optimally directing a satellite during its lifetime, despite all internal and external environmental disturbances and faults [1]. In recent decades, the problem of attitude control for rigid spacecraft has become an active research field due to its significant applications, such as aerial photography, weather forecasting, and remote sensing [2,3]. However, the attitude dynamics are nonlinear, highly complex, and subject to external disturbances and uncertainties. Therefore, research in the field of satellite attitude control has increased to ensure the stability and high reliability of satellites.

Due to the high cost of launch and maintenance, reliability is one of the most important considerations in the design of an attitude control system. Actuator faults clearly reduce the performance of the control system and may even lead to its instability. Therefore, in recent years, the use of fault-tolerant control (FTC) methods in satellite attitude control systems has been emphasized [4-7].

In general, FTC methods can be divided into two categories: passive and active fault-tolerant control. The passive FTC method can handle various faults, but its fault tolerance often comes at the cost of system performance. Hence, active FTC is used to overcome these disadvantages. The active FTC method includes a fault detection and diagnosis (FDD) module that detects and identifies faults and failures in real-time. By reconfiguring the controller, it actively responds to the faults in the control system. Sliding mode observers are commonly used to detect and identify faults in spacecraft [8-10], [9].

* Corresponding author
*E-mail address:* m_nourimanzar@sbu.ac.ir
https://orcid.org/0000-0002-5443-0028
http://dx.doi.org/10.48308/ijrtei.2025.237901.1069

Several methods have been proposed for designing attitude control, with the sliding mode control (SMC) method being the most common [11-14]. SMC and its variations, such as terminal sliding mode control (TSMC), have been studied and applied due to their superior properties, including fast and highly accurate tracking [15]. However, TSMC has some disadvantages, such as singularity and chattering. To avoid singularity, TSMC-based controllers like non-singular TSMC (NTSMC), which also operates in finite-time, have been utilized in spacecraft [16,17]. TSMCs are suitable for second-order systems and certain classes of higher-order systems. Therefore, a universal NTSMC method was proposed to ensure the finite-time stability of nonlinear systems while avoiding singularities [18].

To address the chattering problem, various approaches have been proposed, including boundary layer methods, high-order SMC-based methods, and sliding mode control with adaptive switching gain [19-26]. However, sliding mode control with adaptive switching gain does not completely solve the chattering problem. Therefore, in this paper, we propose the super-twisting non-singular terminal sliding mode control, which significantly reduces chattering, has no singularity issues, and is also suitable for high-order systems [7].

To increase the reliability of spacecraft, enhance maneuverability, and make the system fault-tolerant, spacecraft are usually equipped with additional actuators (more than three). Using command allocation (CA) techniques, a desirable control goal is achieved by appropriately distributing control commands to each actuator [27,28].

In this paper, we apply a proposed super-twisting sliding mode controller to the attitude dynamics of satellites, which are affected by disturbances and uncertainties. The actuators are four reaction wheels with a pyramidal configuration that are subjected to loss of effectiveness faults as well as failure. To estimate the faults, a sliding mode observer is used. In addition, a command allocation (CA) algorithm is employed to properly distribute the control commands. Using the proposed method, chattering and singularity problems are solved, and finite-time convergence is achieved.

The paper is organized as follows: Section 2 presents satellite kinematic and dynamic models, along with the dynamics model of reaction wheels (RWs). In Section 3, an adaptive sliding mode observer is proposed to estimate actuator faults. A super-twisting sliding mode fault-tolerant controller is designed in Section 4. Section 5 presents an optimal command allocation. In Section 6, the simulation results are provided to evaluate the performance of the proposed method, and finally, Section 7 concludes the study.

## 2. Dynamics Model of the Satellite Attitude and Reaction Wheels

In this section, we describe the kinematics and dynamics of the spacecraft attitude. The kinematic model of the spacecraft using modified Rodriguez parameters (MRP) is described as follows [18]:

$$\dot{\rho} = \left[ \frac{I - \rho^{\times} + \rho\rho^{T} - \frac{(1+\rho^{T}\rho)I}{2}}{2} \right] \omega, \qquad (1)$$

where $\rho \in {\sim}^{3\times1}$ indicates the attitude of MRPs of the spacecraft and $\omega \in {\sim}^{3\times1}$ is the angular velocity vector of the satellite expressed in the body coordinate system relative to inertia. Moreover, $I$ denotes the identity matrix with dimensions 3 by 3, and $\rho^{\times}$ denotes skew symmetric matrix of a given vector $\rho$:

$$\rho^{\times} = \begin{bmatrix} 0 & -\rho_3 & \rho_2 \\ \rho_3 & 0 & -\rho_1 \\ -\rho_2 & \rho_1 & 0 \end{bmatrix}.$$

Also, the satellite attitude dynamics model is:

$$J_s\dot{\omega} = -\omega^{\times} J_s \omega + u + d, \qquad (2)$$

where $\omega$ is the angular velocity of the satellite, $J_s$ is the inertial matrix of the satellite, $u$ is the control torque produced by the actuators, and $d$ represents the external disturbances and $\omega^{\times}$ denotes skew symmetric matrix of a given vector $\omega$:

$$\omega^{\times} = \begin{bmatrix} 0 & -\omega_3 & \omega_2 \\ \omega_3 & 0 & -\omega_1 \\ -\omega_2 & \omega_1 & 0 \end{bmatrix}.$$

If the satellite actuators are four reaction wheels, the dynamics equations of the satellite attitude along with $\dot{h}_w = \tau_d$, the reaction wheels are modeled as follows [19], and [26]:

$$J_s\dot{\omega} = -\omega^{\times}(J_s\omega + D\,h_w) + D\tau_d + d, \qquad (3)$$

$$\dot{h}_w = \tau_d, \qquad (4)$$

where $D$ is the distribution matrix, $\tau_d$ is the generated torque of the wheel and $h_w$ is the angular momentum of the reaction wheel. Also, the angular momntem is related to angular velocity as

$$h_w = J_w \omega_w, \qquad (5)$$

where $J_w$ is the inertia matrix of the reaction wheel, and $\omega_w$ is the angular velocity of the wheel. Now, considering faults, the attitude dynamics (3) is modified as follows:

$$J_s\dot{\omega} = -\omega^{\times}(J_s\omega + DJ_w\omega_w) + D(E\tau_d + \overline{\text{v}}) + d, \qquad (6)$$

where $E$ is the loss of effectiveness matrix, and $\overline{\text{v}}$ is the bias fault. $d$ is denoted as the disturbance torque. The matrix $E$ is as follows:

$$E = diag(e_{ii}), \qquad (7)$$

which for a satellite with 4 reaction wheels is shown as follows:
$E = diag(e_{11}, e_{22}, e_{33}, e_{44})$,
where $e_{ii} = 1$ means that the $i$ th actuator is healthy, $0 < e_{ii} < 1$ shows a loss of effectiveness, and $e_{ii} = 0$ means the $i$ th actuator is completely failed. Additionally, we define a new variable as follows $\bar{d} \triangleq D\overline{\nu} + d$.

**Assumption 1.** The control torque provided by the actuators is bounded, *i.e* $|\tau_d| \le \tau_{\max}$, where $\tau_{\max}$ is a positive constant.

**Assumption 2.** The nonlinear function $\omega^{\times} J\omega$ is the 1st order Lipschitz function with a Lipschitz constant $\varepsilon$, which is formulated as follows:

$$\left\|\omega^{\times} J\omega - \hat{\omega}^{\times} J\hat{\omega}\right\| \le \varepsilon \left\|\tilde{\omega}\right\|, \tag{8}$$

$\hat{\omega}$ is the estimation of $\omega$, and $\tilde{\omega} \triangleq \omega - \hat{\omega}$.

**Assumption 3.** Disturbances are bounded with a non-negative constant $d_M$ as $\|d\| \le d_M$.

## 3. Adaptive Sliding Mode Observer

In this section, by assuming that there exist sensors to measure the angular velocity of the satellite $\omega$, an adaptive sliding mode observer is used to estimate the loss of effectiveness $e$, and bias fault $\overline{\nu}$. To this aim an estimation of $\hat{\omega}$ is also required to have a criteria for the error of faults estimations. $\hat{\omega}$ is also derived by an observer.

Since $E$ is a diagonal matrix, the term $E\tau_d$ is written as follows:
$E\tau_d = Te$,
where $T = diag(\tau_{d_1}, \tau_{d_2}, \tau_{d_3}, \tau_{d_4})$ and $e = [e_{11}\ e_{22}\ e_{33}\ e_{44}]^T$. Therefore, the dynamics (6) is rewritten as follows:

$$\dot{\omega} = -J_s^{-1}\omega^{\times}(J_s\omega + DJ_w\omega_w) + J_s^{-1}DTe + J_s^{-1}D\overline{\nu} + J_s^{-1}d. \tag{9}$$

Now, to estimate the angular velocity of the satellite $\hat{\omega}$, an adaptive sliding mode observer is proposed in [9] as follows:

$$\dot{\hat{\omega}} = \Delta(\omega - \hat{\omega}) - J_s^{-1}\hat{\omega}^{\times}(J_s\hat{\omega} + DJ_w\omega_w) + J_s^{-1}DT\hat{e} + J_s^{-1}D\hat{\overline{\nu}} + J_s^{-1}f(t)sign(\tilde{\omega}), \tag{10}$$

where $\tilde{\omega} \triangleq \omega - \hat{\omega}$, $\Delta$ is a predetermined diagonal matrix, such that $\lambda_{\min}(\Delta) - \varepsilon\left\|J_s^{-1}\right\| \ge 0$, and $f(t)$ is a positive time-varying function defined as:

$$\dot{f}(t) = \begin{cases} \gamma_3 \left\|J_s^{-1}\right\|\left\|\tilde{\omega}\right\| sign(\left\|\tilde{\omega}\right\| - \in) & if\ f > \eta \\ \eta & if\ f \le \eta \end{cases} \tag{11}$$

where $\in$ and $\eta$ are small positive constants, $\gamma_3$ is also greater than zero, so that $f(t)$ becomes non-negative. Using (9) and (10), we have:

$$\dot{\tilde{\omega}} = -\Delta\tilde{\omega} - J_s^{-1}(\omega^{\times}J_s\omega - \hat{\omega}^{\times}J_s\hat{\omega}) + J_s^{-1}DT\tilde{e} + J_s^{-1}D\tilde{\overline{\nu}} + J_s^{-1}d - J_s^{-1}f(t)sign(\tilde{\omega}) \tag{12}$$

where $\tilde{e} \triangleq e - \hat{e}$, and $\tilde{\overline{\nu}} \triangleq \overline{\nu} - \hat{\overline{\nu}}$. The estimations of the loss of effectiveness as well as the bias fault, $\hat{e}$ and $\hat{\overline{\nu}}$ are calculated as following:

$$\dot{\hat{e}} = \gamma_1 T^T D^T J_s^{-T}\tilde{\omega} \tag{13}$$

$$\dot{\hat{\overline{\nu}}} = \gamma_2 D^T J_s^{-T}\tilde{\omega} \tag{14}$$

where $\gamma_1$ and $\gamma_2$ are learning rates which are positive constants.

**Assumption 4.** $f(t)$ is bounded, with a constant $f^*$. In addition, the following conditions are also satisfied:
$\|d\| \le d_M \le f(t) \le f^*$.

**Theorem 1.** ([9]) For the dynamics given in (9), if assumptions (2), (3) and (4) hold, then, the estimations error of the angular velocities, and faults provided by adaptive sliding mode observer (10-14), are stable which means accurate fault estimations are provided.

**Proof.** To prove the stability of the fault observer, we use the Lyapunov function as follows:

$$V_O = \tilde{\omega}^T\tilde{\omega} + \frac{1}{\gamma_1}\tilde{e}^T\tilde{e} + \frac{1}{\gamma_2}\tilde{\overline{\nu}}^T\tilde{\overline{\nu}} + \frac{1}{\gamma_3}(f - f^*)^2 \tag{15}$$

where $\gamma_3$ is a positive constant. By deriving the Lyapunov function, we have:

$$\begin{aligned}\dot{V}_O &= 2\tilde{\omega}^T\dot{\tilde{\omega}} + \frac{2}{\gamma_1}\tilde{e}^T\dot{\tilde{e}} + \frac{2}{\gamma_2}\tilde{\overline{\nu}}^T\dot{\tilde{\overline{\nu}}} + \frac{2}{\gamma_3}(f - f^*)\dot{f} \\ &= 2\tilde{\omega}^T(-\Delta\tilde{\omega} - J_s^{-1}(\omega^{\times}J_s\omega - \hat{\omega}^{\times}J_s\hat{\omega}) + J_s^{-1}DT\tilde{e} \\ &\quad + J_s^{-1}D\tilde{\overline{\nu}} + J_s^{-1}d - J_s^{-1}f(t)sign(\tilde{\omega})) - \frac{2}{\gamma_1}\tilde{e}^T\dot{\hat{e}} \\ &\quad - \frac{2}{\gamma_2}\tilde{\overline{\nu}}^T\dot{\hat{\overline{\nu}}} + \frac{2}{\gamma_3}(f - f^*)\dot{f}\end{aligned} \tag{16}$$

From Assumption 2,3, and 4, and using equations (11), (13), and (14), for the case $f > \eta$, we have:

$$\begin{aligned}\dot{V}_O &\le (-2\lambda_{\min}(\Delta) + 2\left\|J_s^{-1}\right\|\varepsilon)\left\|\tilde{\omega}\right\|^2 + 2\left\|\tilde{\omega}^T\right\|\left\|J_s^{-1}\right\|(d_M - f^*) \\ &\quad - (f - f^*)(-2\left\|J_s^{-1}\right\|\left\|\tilde{\omega}\right\| sign(\left\|\tilde{\omega}\right\| - \in) + 2\left\|\tilde{\omega}^T\right\|\left\|J_s^{-1}\right\|)\end{aligned} \tag{17}$$

For the case $\|\tilde{\omega}\| \ge \in$, the last term of (17),

$\xi \triangleq -2\|J_s^{-1}\|\|\tilde{\omega}\| sign(\|\tilde{\omega}\| - \epsilon) + 2\|\tilde{\omega}^T\|\|J_s^{-1}\|$
is zero and from Assumption 5, we have:

$$\dot{V}_O \le (-2\lambda_{\min}(\Delta) + 2\|J_s^{-1}\|\varepsilon)\|\tilde{\omega}\|^2 \quad (18)$$

Therefore, due to $\lambda_{\min}(\Delta) - \varepsilon\|J_s^{-1}\| \ge 0$, we have $\dot{V}_O \le 0$. For the other case $\|\tilde{\omega}\| < \epsilon$, the inequality (17) results in $\dot{V}_O \le 0$, due to $\lambda_{\min}(\Delta) - \varepsilon\|J_s^{-1}\| \ge 0$, and Assumption 5. Therefore, stability of the estimation errors is proved.
Additionally, for the case $f \le \eta$, according to equation (16) with substituting equations (13) and (14), we have:

$$\dot{V}_O = 2\tilde{\omega}^T(-\Delta\tilde{\omega} - J_s^{-1}(\omega^{\times} J_s\omega - \hat{\omega}^{\times} J_s\hat{\omega}) + J_s^{-1}d - J_s^{-1}f(t)sign(\tilde{\omega})) + \frac{2}{\gamma_3}(f - f^*)\eta \quad (19)$$

From Assumption 5 and using $\lambda_{\min}(\Delta) - \varepsilon\|J_s^{-1}\| \ge 0$, $\dot{V}_O \le 0$ is concluded and therefore stability of the estimation errors is concluded ■

**Note 1.** The aforementioned adaptive sliding-mode observer, unlike many developed observer design approaches, does not require prior knowledge about uncertainties or disturbances.

## 4. Super Twisting Sliding Mode Controller

For traditional TSMC, there are two weaknesses, singularity and chattering. In order to solve these two problems and also to have higher performance, a super twisting NTSMC is applied. We first give a lemma:
**Lemma 1** [23] Consider the following dynamics:
$\dot{x} = f(x), \quad x \in R.$
The origin is a global finite-time stable equilibrium point if the following two conditions hold:
1. $V_c$, which is a Lyapunov function, is positive definite.
2. $\dot{V}_c \le -\alpha V_c^{\beta}$, where $\alpha > 0$, and $\beta \in (0,1)$.
We first define a traditional terminal sliding surface as follows:

$$s = \omega + \beta\rho^{\frac{n}{r}} \quad (20)$$

where $\beta > 0$, and both $n$ and $r$ are positive odd integers which satisfy the condition of $1 < \frac{r}{n} < 2$. By applying an appropriate control, the states of the attitude control system converge from any initial condition along the sliding surface in finite time to their desired equilibrium points ($\rho = 0$, $\omega = 0$). In real engineering applications, the states usually do not reach ideal equilibrium points, but enter a small set that contains the origin, i.e. $\|s\| \le \delta$; $\delta > 0$.
For the satellite whose kinematics and dynamics are given in equations (1) and (6), the following super twisting terminal sliding mode control law is proposed:

$$\tau_d = (DE)^+(\omega^{\times}(J_s\omega + DJ_w\omega_w) - \beta\frac{n}{r}J_s diag(\rho^{\frac{n}{r}-1})\dot{\rho} - k_1|s|^{\frac{1}{2}} sign(s) - \sigma\int_0^t sign(s)dt), \quad (21)$$

where $(.)^+$ represents the pseudo-inverse function of a given matrix, $k_1$ and $\sigma$ are small positive constants.
**Assumption 5.** The rate of disturbances and bias fault is bounded; $\left|\dot{\bar{\bar{D}}}\right| \le g$, where $\bar{\bar{D}}$ is defined as $J_s^{-1}d + J_s^{-1}D\bar{v} = \bar{\bar{D}}$.
**Theorem 2.** For the attitude dynamics of a satellite with four RWs given by (3-6), by using the control law (21), finite stability is guaranteed despite the uncertainty of inertia matrix, external disturbances, and faults, if Assumption 6 is satisfied and there exist symmetric and positive definite matrices $P = P^T > 0$, and $Q_l = Q_l^T > 0$ such that the following LMI holds:

$$\begin{pmatrix} PA + A^T P + Q_l + C^T C & PB \\ B^T P & -1/g^2 \end{pmatrix} < 0 \quad (22)$$

**Proof.** Derivative of the sliding surface (20) and using equation (6), we have:

$$\begin{aligned}\dot{s} &= \dot{\omega} + \beta\frac{n}{r}\dot{\rho} diag(\rho^{\frac{n}{r}-1}) \\ &= J_s^{-1}(D(E\tau_d + \bar{v}) + d - \omega^{\times}(J_s\omega + DJ_w\omega_w)) \\ &+ \beta\frac{n}{r}\dot{\rho} diag(\rho^{\frac{n}{r}-1})\end{aligned} \quad (23)$$

By substituting (6), (21) in (23) we have:

$$\dot{s} = -\hat{k}_1|s|^{\frac{1}{2}} sign(s) - \sigma\int_0^t sign(s)dt + J_s^{-1}(d + D\bar{v}) \quad (24)$$

By defining new variables as follows,

$$\begin{cases} f_1 = s \\ f_2 = -\sigma\int_0^t sign(s)d\tau + \bar{\bar{D}} \end{cases} \quad (25)$$

Equation (24) can be written in state space form as:

$$\begin{cases} \dot{f}_1 = -k_1|f_1|^{1/2} sign(f_1) + f_2 \\ \dot{f}_2 = -\sigma sign(f_1) + \dot{\bar{\bar{D}}} \end{cases} \quad (26)$$

We define additional two new variables as follows:

$$\begin{cases} \Gamma_1 = |f_1|^{1/2} sign(f_1) \\ \Gamma_2 = f_2 \end{cases} \quad (27)$$

Derivative of these variables by substituting equations (26) and (27) are as follows:

$$\dot{\Gamma}_1 = \frac{\dot{f}_1 |f_1|^{1/2} - f_1 (1/2)|f_1|^{-1/2} sign(f_1).\dot{f}_1}{|f_1|}$$
$$= \frac{\left[-k_1 |f_1|^{1/2} sign(f_1) + f_2\right]\left(|f_1|^{1/2} - (1/2)|f_1|^{1/2}\right)}{|f_1|}$$
$$= \frac{1}{|f_1|^{1/2}}\left(-\frac{k_1}{2}|f_1|^{1/2} sign(f_1) + \frac{1}{2} f_2\right)$$
$$= \frac{1}{|\Gamma_1|}\left(-\frac{k_1}{2}\Gamma_1 + \frac{1}{2}\Gamma_2\right) \tag{28}$$

$$\dot{\Gamma}_2 = -\sigma sign(f_1) + \dot{\bar{D}}$$
$$= \frac{1}{|f_1|^{1/2}}\left(-\sigma |f_1|^{1/2} sign(f_1) + |f_1|^{1/2} \dot{\bar{D}}\right)$$
$$= \frac{1}{|\Gamma_1|}\left(-\sigma\Gamma_1 + |\Gamma_1| \dot{\bar{D}}\right) \tag{29}$$

Considering $\Gamma = [\Gamma_1 \quad \Gamma_2]^T$, equations (28) and (29) can be rewritten as follows:

$$\dot{\Gamma} = \frac{1}{|\Gamma_1|}(A\Gamma + B\tilde{D})$$
$$A = \begin{pmatrix} -0.5k_1 & 0.5 \\ -\sigma & 0 \end{pmatrix},$$
$$B = \begin{bmatrix} 0 \\ 1 \end{bmatrix},\; C = \begin{bmatrix} 1 & 0 \end{bmatrix} \tag{30}$$

where $|\Gamma_1| = |f_1|^{1/2}$, and $\tilde{D} = \dot{\bar{D}}|\Gamma_1|$. From Assumption 6, we have:

$$|\tilde{D}| \le g|\Gamma_1| \tag{31}$$

Now consider a positive definite Lyapunov function as follows:

$$V_c = \Gamma^T P \Gamma \tag{32}$$

From (32) we have:

$$\lambda_{\min}(P)\|\Gamma\|^2 \le V \le \lambda_{\max}(P)\|\Gamma\|^2 \tag{33}$$

where $\|\Gamma\|^2 = |f_1| + f_2^2$.

The derivative of the Lyapunov function using equations (30) and (32) is as follows:

$$\dot{V}_C = \frac{1}{|\Gamma_1|}\left[\Gamma^T (PA + A^T P)\Gamma + \Gamma^T PB\tilde{D} + \tilde{D}^T B^T P\Gamma\right] \tag{34}$$

From equation (30), we have:

$$|\tilde{D}(t,\Gamma_1)|^2 \le g^2|\Gamma_1|^2 \le g^2(\Gamma_1^2 + \Gamma_2^2) \tag{35}$$

From equation (35), we conclude:

$$\Gamma^T\Gamma - \frac{1}{g^2}\tilde{D}(t,\Gamma_1) > 0 \tag{36}$$

Using equations (34) and (36), we have:

$$\dot{V}_c \le \frac{1}{|\Gamma_1|}\left[\Gamma^T (PA + A^T P)\Gamma + \Gamma^T PB\tilde{D} + \tilde{D}^T B^T P\Gamma + \Gamma^T\Gamma - \frac{1}{g^2}\tilde{D}^2\right]$$
$$\dot{V}_c \le \frac{1}{|\Gamma_1|}\left[\Gamma^T (PA + A^T P + C^T C + Q_l - Q_l)\Gamma + \Gamma^T PB\tilde{D} + \tilde{D}^T B^T P\Gamma - \frac{1}{g^2}\tilde{D}^2\right]$$

which is written as follows:

$$\dot{V}_c \le \frac{1}{|\Gamma_1|}\begin{bmatrix} \Gamma \\ \tilde{D} \end{bmatrix}^T \begin{pmatrix} PA + A^T P + Q_l + C^T C & PB \\ B^T P & -1/g^2 \end{pmatrix}\begin{bmatrix} \Gamma \\ \tilde{D} \end{bmatrix} - \frac{1}{|\Gamma_1|}\Gamma^T Q_l \Gamma \tag{37}$$

So, the LMI condition is considered as

$$\begin{pmatrix} PA + A^T P + Q_l + C^T C & PB \\ B^T P & -1/g^2 \end{pmatrix} < 0$$

Consequently, based on (33) and (37), we have:

$$\dot{V}_c \le -\frac{1}{|\Gamma_1|}\Gamma^T Q_l \Gamma \le -\frac{1}{|\Gamma_1|}\lambda_{\min}(Q_l)\|\Gamma\|^2 \le -\frac{1}{|\Gamma_1|}\lambda_{\min}(Q_l)\frac{V}{\lambda_{\max}(P)} \tag{38}$$

According to inequality (33), we have:

$$-\frac{1}{|\Gamma_1|} \le -\frac{1}{\|\Gamma\|} \le -\frac{\lambda_{\min}^{\frac{1}{2}}(P)}{V_c^{\frac{1}{2}}} \tag{39}$$

Therefore, from (38) and (39), we have:

$$\dot{V}_c \le -\alpha V_c^{\frac{1}{2}},\; \alpha = \frac{\lambda_{\min}(Q_l)\lambda_{\min}^{\frac{1}{2}}(P)}{\lambda_{\max}(P)} \tag{40}$$

From Lemma 1 the inequality (40) concludes that the angular velocity and attitude of the satellite converge to zero in a finite time ■

**Note 1.** The design of the control law (21) has a problem in its second term that causes the singularity phenomenon. To prevent this phenomenon, we modify the control law (21) as follows:

$$\tau_d = (DE)^+(\omega^\times(J_s\omega + DJ_w\omega_w)) + sat(r_f, r_s) - k_1|s|^{\frac{1}{2}} sign(s) - \sigma\int_0^t sign(s)dt), \quad (41)$$

where

$$sat(r_f, r_s) = \begin{cases} r_s sign(r_f), & |r_f| > r_s \\ r_f, & otherwise \end{cases} \quad (42)$$

and $r_f$ is defined as follows:

$$r_f \triangleq -\beta\frac{n}{r}J_s diag(\rho^{\frac{n}{r}-1})\dot{\rho}. \quad (43)$$

$r_s$ is the upper bound of the saturation function.
The proof and analysis of this modification was given in [19].

## 5. Online closed-loop FTC allocation design with optimization method

Due to the possibility of actuator fault, the proper distribution of the control command between the redundant actuators should be done by the command allocation unit which is calculated by minimizing a cost function as follows

$$D_\tau = \underset{\tau_{\min_i}(t) \le \tau_{act}(t) \le \tau_{\max_i}(t)}{\arg} \min \left\| u_d(t) - D\hat{E}\tau_{act}(t) \right\|$$

where $u_d$ is the desired system control torque, and $\hat{E} = diag(\hat{e})$. $\tau_{act}(t)$ represents the actual actuator torque produced by the reaction wheel.

$\tau_{\min_i}(t); i = 1,...,4$ and $\tau_{\max_i}(t); i = 1,...,4$ are the lower and upper bound of the actuators torques:

$$\tau_{\min_i}(t) = \max\{\tau_i(t)_{\min}, \tau_i(t-T) + T\min\{\eta_{\min}\}\}$$
$$\tau_{\max_i}(t) = \min\{\tau_i(t)_{\max}, \tau_i(t-T) + T\max\{\eta_{\max}\}\}$$

where $\eta_{\min}$, $\eta_{\max}$ denote the minimum and maximum actuator rates, respectively.
This optimization problem minimizes the distance between the desired control signal and the torques provided by the all actuators. This is done by distributing the signal between the actuators based on their healthiness ($\hat{E}$) and the distribution matrix, $D$.
For example, if the $i^{\text{th}}$ actuator is failed $e_{ii} = 0$, or it has loss of effectiveness $e_{ii} < 0$, then the control signal is rerouted and distributed to other actuators to compensate this fault and therefore the other actuators produce more torques.
In addition of the mention cost function, another cost function can also be selected such that the energy consumption is also minimized and from the actuators saturation is prevented. Therefore, we consider the cost function as follows [23]:

$$J = \underset{\tau_{act} \in D_\tau}{\arg} \min\{\|W_0\tau_{act}(t)\|^2 + \|W_1(\tau_{act}(t) - \tau_d(t))\|^2 + \|W_2(\tau_{act}(t) - \tau_{act}(t-T))\|^2\} \quad (49)$$

$\tau_d$ is the desired actuator torque, that is, when the actuators are all healthy. $T$ is the sampling time, and $W_0$, $W_1$, and $W_2$ are weight matrices.
In the case of failure or fault of the $i^{\text{th}}$ RWs, $\tau_{act}(t)$ is redirected or distributed to other actuators. Moreover, the control torques quickly converge to the desired command when choosing a large $W_1$. In addition, if $W_2$ is large, the response of the actuators will be smooth.
Solving the optimization problem, the optimal CA solution is obtained as follows:

$$\tau_{act}(t) = M\tau_d(t-T) + L\tau_d(t) + N\tau_{act}(t-T),$$

where $M = (I - LD\hat{E})Q^{-2}(P_1W_1)^2$, and $N = (I - LD\hat{E})Q^{-2}W_2^2$, and $L = Q^{-1}(D\hat{E}Q^{-1})^+$. In addition, $Q = \left(\left(P_0(\hat{E} + \delta_e I)^{-1}\right)^2 + (P_1W_1)^2 + W_2^2\right)^{1/2}$, and $P_0$ and $P_1$ are auxiliary matrices.

## 6. Simulation results

In this section, we examine the performance of the proposed method applied to satellite attitude control in the presence of external disturbances, uncertainty in the inertia matrix, and the simultaneous loss of effectiveness in the actuators in two scenarios. Since our method extends the method NTSMC proposed in [18], the results are compared with.
The spacecraft actuators are four RWs which are configured as a pyramid. The maximum torque of each RW is $\tau_{\max} = 0.6\,N.m.$ Assembly angles are $\alpha_4 = 35.26$ deg, and $\beta_4 = 45$ deg. The upper bound of the angular velocity and its rate for each wheel are $4000\,rpm$ and $12.5\,rad/s^2$, respectively. The inertia matrix and its uncertain part are as follows:

$$J = \begin{bmatrix} 20 & 0 & 0.9 \\ 0 & 17 & 0 \\ 0.9 & 0 & 15 \end{bmatrix}, \Delta J = \begin{bmatrix} 2.5 & 0 & 0 \\ 0 & 2 & 0 \\ 0 & 0 & 1.5 \end{bmatrix}.$$

External disturbances are also considered as follows:

$$d = 0.2\times 10^{-3}\begin{bmatrix} 3\cos(100\|\omega\|t) + 4\sin(30\|\omega\|t) - 10 \\ -1.5\sin(20\|\omega\|t) + 3\cos(50\|\omega\|t) + 15 \\ 3\sin(100\|\omega\|t) - 8\sin(30\|\omega\|t) + 10 \end{bmatrix}.$$

Satellite initial angular velocities and Euler angles are $\omega_0 = (0.2, 0.2, 0.2)^T$ deg/sec, and

$(roll, pitch, yaw) = (33.10, 35.16, 12.09)$ deg, respectively.

Scenario 1: A loss of effectiveness in the first wheel and a complete failure of the reaction wheel in the second actuator occurred at the same time, which are as follows:

$$e_{11} = \begin{cases} 1, & t < 60 \\ 0.5, & t \geq 60 \end{cases}, \quad e_{22} = \begin{cases} 1, & t < 60 \\ 0, & t \geq 60 \end{cases}$$

The simulation results are presented in Fig. 1-4. As shown in Fig. 1, the actuator faults are estimated with high precision which means the applied observer works properly. Fig. 2 illustrates the attitude of the satellite based on Modified Rodrigues Parameters using both the NTSMC method [18] and the proposed super-twisting non-singular terminal sliding mode control. From the left figure, it is seen that the proposed method is faster than NTSMC and its transition response is better. The right figure which is the results between 600-1000 seconds shows more accurate regulation is achieved by the proposed method Fig. 3 and 4 depict the regulation of the satellite's angular velocities, demonstrating that the proposed super-twisting NTSMC method outperforms the NTSMC method [18] in terms of accuracy and reduced chattering. Fig. 4 shows the reaction wheel torques, which remain within their specified limits and it is seen our proposed method reduces the chattering significantly.

Scenario 2: In another simulation, a loss of effectiveness in the first wheel, a complete failure of the second reaction wheel, and a loss of effectiveness in the third wheel occurred at different times as follows:

$$e_{11} = \begin{cases} 1, & t < 60 \\ 0.5, & t \geq 60 \end{cases}, \quad e_{22} = \begin{cases} 1, & t < 60 \\ 0, & t \geq 60 \end{cases}$$

$$e_{33} = \begin{cases} 1 & t \leq 5 \\ 0.5 & t > 5 \end{cases}.$$

Fig. 5 depicts the regulation of the satellite's angular velocities of the proposed super-twisting NTSMC method compared with NTSMC method [18]. As seen, the results from the proposed method is faster. Fig. 6 shows the command allocation between the four reaction wheels. This figure shows that the torques provided by the actuators are changed when a fault is accrued (t=60s). According to the figure, the chattering has significantly decreased compared to the NTSMC method [18].

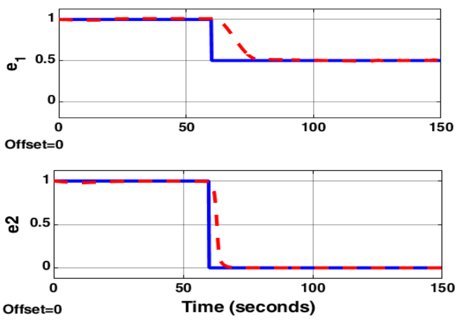


**Fig 1.** Estimating of the loss of effectiveness Blue diagram: fault, red diagram: estimated fault (Scenario 1)

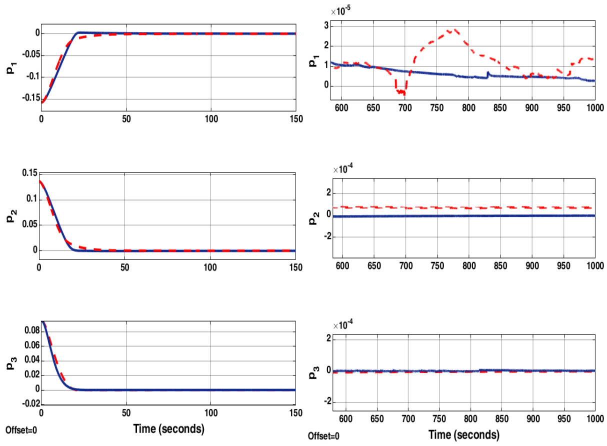


**Fig 2.** Satellite attitude based on modified Rodrigues parameters in scenario 1. Blue diagram: proposed method, red diagram: NTSMC method [18] (Scenario 1)

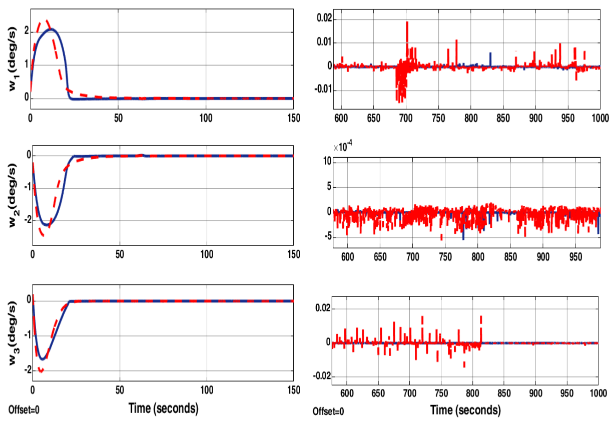


**Fig 3.** Angular velocities of the satellite in scenario 1. Blue diagram: proposed method, red diagram: NTSMC. [18] (Scenario 1)

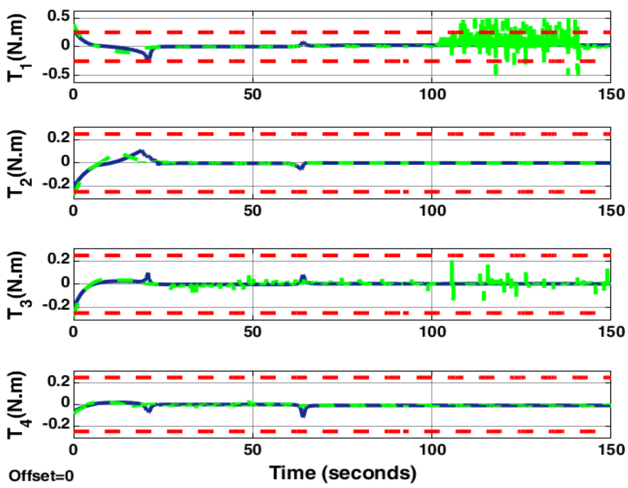


**Fig 4.** Reaction wheels' torques in scenario 1. Blue diagram: proposed method, green diagram: NTSMC [18]. (Scenario 1)

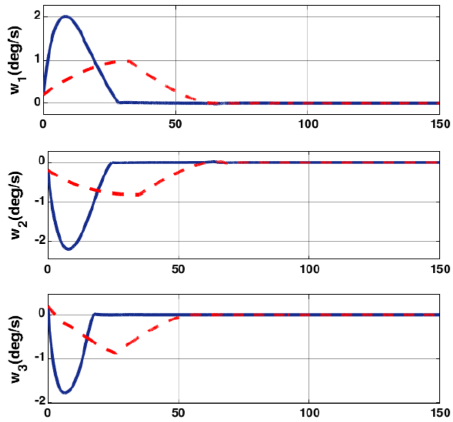


**Fig 5.** Angular velocities of the satellite in scenario 2. Blue diagram: the proposed method, red diagram: NTSMC [18]. (Scenario 2)

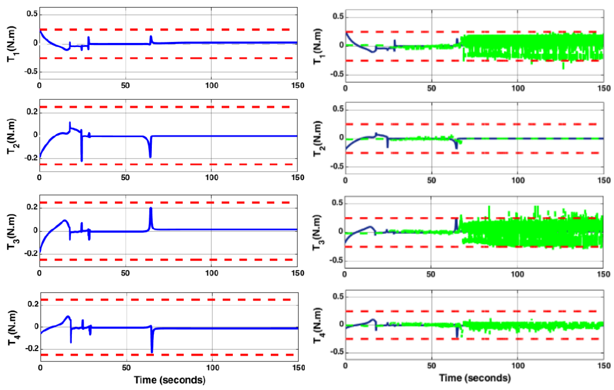


**Fig 6.** Reaction wheels' torques in scenario 1. Blue diagram: proposed method, green diagram: NTSMC. (Scenario 2)

## 7. Conclusion

In this paper, we proposed a finite-time attitude control method using a super-twisting adaptive sliding mode for a satellite with four reaction wheels. To increase the accuracy of the controller, the dynamics of the reaction wheels were also incorporated into the attitude dynamics model. The stability of the super-twisting adaptive NTSM fault-tolerant controller, in the presence of uncertainties in the inertia matrix, external disturbances, and two types of faults (loss of effectiveness fault and bias fault), was proved using the Lyapunov method. An adaptive sliding mode observer was employed to estimate actuator faults, and its stability was verified. Additionally, a command allocation (CA) technique was applied to optimally distribute the commands among the actuators. The results show that, compared to traditional methods like the NTSMC method, higher performance in terms of reducing chattering phenomena and improving accuracy in regulating to the desired attitude in finite time was achieved.

## References

[1] W. Ley, K. Wittmann, and W. Hallmann, Handbook of space technology. John Wiley & Sons, 2009.

[2] J. R. Kopacz, R. Herschitz, and J. Roney, "Small satellites an overview and assessment," *Acta Astronautica*, vol. 170, pp. 93–105, 2020.

[3] M. Sorek-Hamer, A. C. Just, and I. Kloog, "Satellite remote sensing in epidemiological studies," *Current opinion in pediatrics*, vol. 28, no. 2, pp. 228–234, 2016.

[4] Q. Shen, C. Yue, C. H. Goh, and D. Wang, "Active fault-tolerant control system design for spacecraft attitude maneuvers with actuator saturation and faults," *IEEE Transactions on Industrial Electronics*, vol. 66, no. 5, pp. 3763–3772, 2018.

[5] M. N. Hasan, M. Haris, and S. Qin, "Fault-tolerant spacecraft attitude control: A critical assessment," *Progress in Aerospace Sciences*, vol. 130, p. 100806, 2022.

[6] .F. A. N. Liming, H. Huang, and Z. Kaixing, "Robust fault-tolerant attitude control for satellite with multiple uncertainties and actuator faults," *Chinese Journal of Aeronautics*, vol. 33, no. 12, pp. 3380–3394, 2020.

[7] L. Ashayeri, A. Doustmohammadi, and F. Fani Saberi, "Adaptive Fault-Tolerant Control Allocation of Flexible Satellite with Infinite-Dimensional Model," *J. Aerosp. Eng.*, vol. 35, no. 4, p. 04022040, Jul. 2022,

[8] D. Efimov, C. Edwards, and A. Zolghadri, "Enhancement of adaptive observer robustness applying sliding mode techniques," *Automatica*, vol. 72, pp. 53–56, 2016.

[9] X. Zhang, Z. Gao, M. Qian, and L. Bai, "Integrated fault estimation and fault-tolerant control for rigid spacecraft attitude system with multiple actuator faults," *International Journal of Innovative Computing, Information and Control*, vol. 15, no. 4, pp. 1255–1270, 2019.

[10] L. Gou, Y. Shen, H. Zheng, and X. Zeng, "Multi-fault diagnosis of an aero-engine control system using joint sliding mode observers," *IEEE Access*, vol. 8, pp. 10186–10197, 2020.

[11] Y. Miao, I. Hwang, M. Liu, and F. Wang, "Adaptive fast nonsingular terminal sliding mode control for attitude tracking of flexible spacecraft with rotating appendage," *Aerospace Science and Technology*, vol. 93, p. 105312, 2019.

[12] S. M. Esmaeilzadeh, M. Golestani, and S. Mobayen, "Chattering-free Fault-tolerant Attitude Control with Fast Fixed-time Convergence for Flexible Spacecraft," *Int. J. Control Autom. Syst.*, vol. 19, no. 2, pp. 767–776, Feb. 2021.

[13] B. Hang, B. Su, and W. Deng, "Adaptive sliding mode fault-tolerant attitude control for flexible satellites based on ts fuzzy disturbance modeling," *Math. Biosci. Eng*, vol. 20, pp. 12700–12717, 2023.

[14] Q. Yao, H. Jahanshahi, S. Bekiros, S. F. Mihalache, and N. D. Alotaibi, "Indirect neural-enhanced integral sliding mode control for finite-time fault-tolerant attitude tracking of spacecraft," *Mathematics*, vol. 10, no. 14, p. 2467, 2022

[15] S. Murugesan and P. S. Goel, "Fault-tolerant spacecraft attitude control system," *Sadhana*, vol. 11, no. 1–2, pp. 233–261, Oct. 1987, doi: 10.1007/BF02811321.

[16] B. Xiao, Q. Hu, Y. Zhang, and X. Huo, “Fault-Tolerant Tracking Control of Spacecraft with Attitude-Only Measurement Under Actuator Failures,” *Journal of Guidance, Control, and Dynamics*, vol. 37, no. 3, pp. 838–849, 2014,

[17] Y. Feng, M. Zhou, X. Zheng, F. Han, and X. Yu, “Full-order terminal sliding-mode control of MIMO systems with unmatched uncertainties,” *Journal of the Franklin Institute*, vol. 355, no. 2, pp. 653–674, 2018.

[18] Y. Feng, X. Yu, and F. Han, “On nonsingular terminal sliding-mode control of nonlinear systems,” *Automatica*, vol. 49, no. 6, pp. 1715–1722, 2013.

[19] F. L. Markley and J. L. Crassidis, “Attitude Control,” in *Fundamentals of Spacecraft Attitude Determination and Control*, New York, NY: Springer New York, 2014, pp. 287–343.

[20] Q. Hu, B. Li, B. Xiao, and Y. Zhang, “Nonlinear Proportional-Derivative Control Incorporating Closed-Loop Control Allocation for Spacecraft,” in *Control Allocation for Spacecraft Under Actuator Faults*, Singapore: Springer Singapore, 2021, pp. 157–183.

[21] G. Kopp and J. L. Lean, “A new, lower value of total solar irradiance: Evidence and climate significance: FRONTIER,” *Geophys. Res. Lett.*, vol. 38, no. 1, Jan. 2011,

[22] B. Li, Q. Hu, G. Ma, and Y. Yang, “Fault-tolerant attitude stabilization incorporating closed-loop control allocation under actuator failure,” *IEEE Transactions on Aerospace and Electronic Systems*, vol. 55, no. 4, pp. 1989–2000, 2018.

[23] A. Li, M. Liu, and Y. Shi, “Adaptive sliding mode attitude tracking control for flexible spacecraft systems based on the Takagi-Sugeno fuzzy modelling method,” *Acta Astronautica*, vol. 175, pp. 570–581, 2020.

[24] L. Wang, Y. Sheng, and X. Liu, “A novel adaptive high-order sliding mode control based on integral sliding mode,” *Int. J. Control Autom. Syst.*, vol. 12, no. 3, pp. 459–472, Jun. 2014,

[25] D. Zholtayev, M. Rubagotti, and T. D. Do, “Adaptive super-twisting sliding mode control for maximum power point tracking of PMSG-based wind energy conversion systems,” *Renewable Energy*, vol. 183, pp. 877–889, 2022.